# Isotope-Shift Measurement of Bosonic $Yb^+$ Ions

Hong-Ling Yue(乐虹伶)[1,2,3], Hu Shao(邵虎)[1,3*], Zheng Chen(陈正)[1,2,3], Peng-Cheng Fang(方鹏程)[1,3], Meng-Yan Zeng(曾孟彦)[1,2,3], Bao-Lin Zhang(张宝林)[1,3], Yao Huang(黄垚)[1,3], Ji-Guang Li(李冀光)[4], Qun-Feng Chen(陈群峰)[1,3], Hua Guan(管桦)[1,3,7*], and Ke-Lin Gao(高克林)[1,3,5,6*]

[1]*State Key Laboratory of Magnetic Resonance and Atomic and Molecular Physics, Innovation Academy of Precision Measurement Science and Technology, Chinese Academy of Sciences, Wuhan 430071, China*
[2]*University of the Chinese Academy of Sciences, Beijing 100049, China*
[3]*Key Laboratory of Atomic Frequency Standards, Innovation Academy of Precision Measurement Science and Technology, Chinese Academy of Sciences, Wuhan 430071, China*
[4]*Institute of Applied Physics and Computational Mathematics, Beijing 100088, China*
[5]*Hefei National Research Center for Physical Sciences at the Microscale and School of Physical Sciences, University of Science and Technology of China, Hefei 230026, China*
[6]*CAS Center for Excellence in Quantum Information and Quantum Physics, University of Science and Technology of China, Hefei 230026, China*
[7]*Wuhan Institute of Quantum Technology, Wuhan 430206, China*

(Received 18 March 2023; accepted manuscript online 23 August 2023)

We present a method that the atomic transition frequency measurement relies on the accurate wavemeter, optical frequency comb and stable Fabry–Pérot cavity to precise determination of stable even isotope shift on single $Yb^+$ ion ($A$ = 168, 170, 172, 174, 176). The $6s\,^2S_{1/2} \leftrightarrow 6p\,^2P_{1/2}$ and $5d\,^2D_{3/2} \leftrightarrow 6s\,^3[3/2]_{1/2}$ resonance dipole transition frequencies are preliminarily measured by using a wavemeter which is calibrated by the 729 nm clock laser of $^{40}Ca^+$. Meanwhile, those frequencies are double checked by using optical frequency comb for correction of deviation. Ultimately, by changing frequency locking points at an ultralow expansion cavity more slightly and monitoring the corresponding atomic fluorescence changing with 17%, we finally improve the resonant frequency uncertainty to ±6 MHz, which is one order of improvement in precision higher than previously published measurements on the same transitions. A King-plot analysis with sensitivity to coupling between electrons and neutrons is carried out to determine the field and mass shift constants. Our measurement combined with existing or future isotope shift measurements can be used to determine basic properties of atomic nuclei, and to test new forces beyond the Standard Model.

DOI: 10.1088/0256-307X/40/9/093202

Isotope shift (IS), which provides a benchmark for understanding atomic and nuclear structures, has been studied for decades.[1–17] IS is mainly caused by small perturbations in the electron transition due to variations in the mass and size/shape of nuclei of different isotopes. Thus, accurate isotope shift measurements provide high-precision tests for relativistic many-body physics used to calculate the electron wave functions and pave the way for the further exploration of nuclear structure theory.[3–6] Measurements have been made for many physical systems, such as $Ca^+$,[4,7–10] $Ba^+$,[11,12] $Sr^+$,[13,14] $Yb^+$,[15,16] and Yb.[17] In the above-mentioned measurements, quite a lot methods have been used, such as (quasi) simultaneous collinear and anticollinear laser spectroscopy,[12] quantum-shelving spectroscopy,[13] photon recoil spectroscopy technique,[8] direct frequency-comb Raman spectroscopy,[10] decoherence free subspaces and two-isotope entangled technique,[14] Doppler-free two-photon spectroscopy.[17]

Within the measurement uncertainty, almost all existing measurements in zero nuclear spin isotopes follow a linear relationship in King-plot analysis.[4,7–14] However, recent work has demonstrated King's nonlinearities. Experimentally, Counts *et al.*[15] demonstrated deviation from linearity at the $3\sigma$ level on the $S_{1/2} \leftrightarrow D_{3/2}$ and $S_{1/2} \leftrightarrow D_{5/2}$ clock transitions of $Yb^+$ by $\sim$300 Hz. Figueroa *et al.*[17] measured IS for the five spinless neutral Yb isotopes on the $6s^2\,^1S_0 \leftrightarrow 5d6s\,^1D_2$ transition, showing that the observed nonlinearity in the joint Yb/$Yb^+$ King-plot analysis can be accounted for the deformation of the Yb nuclei by combining with the results of Counts *et al.*[15] Hur *et al.*[16] performed measurement on the highly forbidden $^2S_{1/2} \leftrightarrow {}^2F_{7/2}$ octupole clock transition of $^{168,170,172,174,176}Yb^+$ ions and found that there is a second distinct source of nonlinearity with $4.3\sigma$ confidence. Theoretically, Allehabi *et al.*[18] predicted that nuclear deformation as a source of the nonlinearity of the King plot in the $Yb^+$ ion, which is consistent with the nonlinearity

*Corresponding authors. Email: shaohu@apm.ac.cn; guanhua@apm.ac.cn; klgao@apm.ac.cn
© 2023 Chinese Physical Society and IOP Publishing Ltd

observed by Counts *et al.*[15]

In general, the higher-order effects under the Standard Model (SM) and new physics beyond the SM are two sources of this nonlinearity, and the latter may be the existence of a spin-independent fifth force that couples neutrons and electrons, adding the IS with another contribution.[4,19] Therefore, high-precision measurement is required to distinguish the sources of King's nonlinearity so that we can set more stringent bounds between the SM and new physics.[10]

Duo to the fact that $Yb^+$ ions involve seven stable isotopes[20] ($A$ = 168, 170, 171, 172, 173, 174, 176) and five of them are nuclear spin-zero, which lack of hyperfine interactions known as the source of King's nonlinearity, thus suitable for search of King's nonlinearity. The $Yb^+$ energy-level diagram of low-lying states are shown in Fig. 1. $E1$ transitions with the wavelengths 369 nm and 935 nm are used for the direct cooling and repumping. $E2$ (436 nm) and $E3$ (467 nm) as clock transitions are used for the precise quantum coherent operations that have met one of the key requirements for breaking nonlinearity with a relative uncertainty of $10^{-15}$ or below,[14] which has confirmed King's nonlinearity in the recent work.[15–17] As for the $6s\,^2S_{1/2} \leftrightarrow 6p\,^2P_{1/2}$ and $5d\,^2D_{3/2} \leftrightarrow 6s\,^3[3/2]_{1/2}$ transitions, Hur *et al.*[16] and McLoughlin *et al.*[21] have made IS measurements by using WS7 wavemeter with the accuracy of 60 MHz. In this Letter, we present a more precise measured value by using optical frequency comb and ultralow expansion (ULE) cavity to double check frequency in the correction of deviation. By changing frequency locking points at a ULE cavity or a wavemeter by ±6 MHz, the corresponding atomic fluorescence changing obviously with $\Delta N/N \approx 17\%$. The result represents one order of improvement in precision than previously published measurements on the same transitions. Besides, we have performed a King plot analysis and extracted constants related to the field and mass shifts.

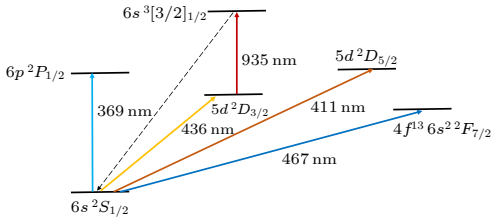


**Fig. 1.** $Yb^+$ relevant energy-level diagram (not to scale).

*Experimental Setup and Procedure.* The experimental setup is depicted in Fig. 2. Our apparatus mainly consists of an ion trap system, a laser system, a WS8-2 wavelength meter, a ULE cavity, a femtosecond-comb (fs-comb), and a field programmable gate array (FPGA), etc.

The ion trap is installed in an ultra-high vacuum chamber with background pressure of less than $1.0 \times 10^{-8}$ Pa to maintain a stable environment for long-lifetime ion trapping. To ensure a more symmetrical structure and to reduce heating effect and micromotion, the trap is made of 0.3-mm-thick rectangular diamond wafer and electrodes are formed by precise laser cutting and gold coating.[22] The fluorescence signal is detected by a photomultiplier tube (PMT). The IS interrogation 369 nm and 935 nm lasers are locked to WS8-2 calibrated by a 729 nm $^{40}Ca^+$ optical clock laser. The locking is completed by the Labview program, the computer extracts the real time measurement frequency from WS8-2 and calculates the feedback voltage value with PID feedback. Then, the National Instruments PCI6733 produces voltage outputs to achieve closed-loop stabilization of the laser frequency.

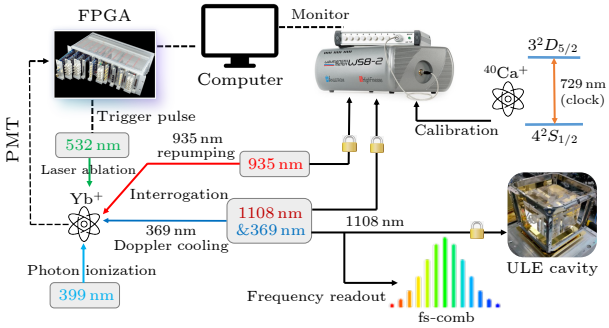


**Fig. 2.** Experimental apparatus for ion loading and IS measurement.

Based on the ablation technique,[23] we use 532 nm, 399 nm, 369 nm and 935 nm diode lasers to load single ytterbium ions. The specific process is depicted as follows: 532 nm pulsed laser is used for sputtering to generate ytterbium atoms, 399 nm laser is used as primary ionization laser to drive ytterbium atom $6s^2\ ^1S_0 \leftrightarrow 6s6p\,^1P_1$ transition, 369 nm is used as secondary ionization laser to realize the ionization of ytterbium atom. The ionized ytterbium ions are Doppler cooled by 369 nm laser, and 935 nm laser maintains ion cooling cycle. In our measurement, we use 369 nm laser and 935 nm laser to drive $6s^2S_{1/2} \leftrightarrow 6p\,^2P_{1/2}$ and $5d\,^2D_{3/2} \leftrightarrow 6s\,^3[3/2]_{1/2}$ transitions, respectively, to measure IS. Typically, 30 μW of 369 nm light (5 μW of 935-nm light) is focused to a waist of 46 μm (135 μm) at the location of the ion. Using the ablation technique and adjusting the corresponding wavelengths of 399 nm, 369 nm, 935 nm lasers, the independent $^{168}Yb^+$, $^{170}Yb^+$, $^{172}Yb^+$, $^{174}Yb^+$, and $^{176}Yb^+$ single ions are successfully confined in a miniature four-blade linear Paul trap. The frequencies are monitored by WS8-2, which is calibrated by the 729 nm clock laser of $^{40}Ca^+$ with an accuracy of 1 Hz.[24]

The 1108 nm laser is frequency stabilized to a standard Fabry–Pérot cavity ($F$ = 7500), which is made of ULE according to the Pound–Drever–Hall scheme, with linewidth and drift of about 200 kHz per day. The laser frequency is simultaneously measured by both the WS8-2 and an fs-comb. The relationship between the two readouts is as follows: $f_{\mathrm{WS8-2}} - f_{\mathrm{comb}} = 12$ MHz, thus the 12 MHz calibration is made for IS measurement on the $6s\,^2S_{1/2} \leftrightarrow 6p\,^2P_{1/2}$ transition. On the $5d\,^2D_{3/2} \leftrightarrow 6s\,^3[3/2]_{1/2}$ transition, we still use the readout of WS8-2 since 935 nm is out of range of the fs-comb.

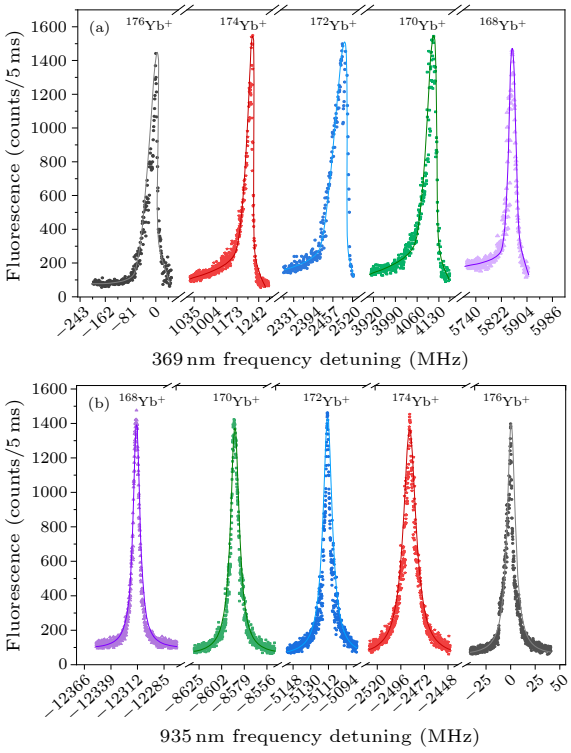


**Fig. 3.** Fluorescence spectra of $^{168}$Yb$^+$, $^{170}$Yb$^+$, $^{172}$Yb$^+$, $^{174}$Yb$^+$, and $^{176}$Yb$^+$ on the $6s\,^2S_{1/2} \leftrightarrow 6p\,^2P_{1/2}$ and $5d\,^2D_{3/2} \leftrightarrow 6s\,^3[3/2]_{1/2}$ transitions. (a) The fluorescence spectra of Yb$^+$ isotopes by scanning 369 nm frequency. (b) The fluorescence spectra of Yb$^+$ isotopes by scanning 935 nm frequency.

Once every single Yb$^+$ isotope is independently loaded, it is cooled to the Lamb–Dick range, then we drive the $6s\,^2S_{1/2} \leftrightarrow 6p\,^2P_{1/2}$ transition by scanning the 369 nm laser frequency and record its corresponding fluorescence with the 935 nm laser frequency at the $5d\,^2D_{3/2} \leftrightarrow 6s\,^3[3/2]_{1/2}$ resonance. The frequency corresponding to the maximum fluorescence is noted as the $6s\,^2S_{1/2} \leftrightarrow 6p\,^2P_{1/2}$ resonance transition frequency. Similarly, we drive the $5d\,^2D_{3/2} \leftrightarrow 6s\,^3[3/2]_{1/2}$ transition by scanning the frequency of 935 nm laser and record its corresponding fluorescence with 369 nm laser frequency at near $6s\,^2S_{1/2} \leftrightarrow 6p\,^2P_{1/2}$ resonance. Through a Lorentzian fitting of fluorescence and its scanning frequencies, we can obtain the $5d\,^2D_{3/2} \leftrightarrow 6s\,^3[3/2]_{1/2}$ resonance transition frequency. During the scanning, 935 nm and 369 nm lasers are locked on WS8-2 so that we can measure the resonance frequency precisely. The frequency-scanning fluorescence spectra of $^{168}$Yb$^+$, $^{170}$Yb$^+$, $^{172}$Yb$^+$, $^{174}$Yb$^+$, and $^{176}$Yb$^+$ on the $6s^2S_{1/2} \leftrightarrow 6p\,^2P_{1/2}$ and $5d\,^2D_{3/2} \leftrightarrow 6s\,^3[3/2]_{1/2}$ transitions are shown in Fig. 3. The scanning of every single Yb$^+$ isotope is repeated for multiple times to determine the central frequency and to reduce its uncertainty.

*Results and Conclusion.* Typically, IS is derived from the mass shift and the field shift. The mass shift is caused by difference in the mass of the nuclei, inducing small shifts in the positions of energy levels, thus causing the frequency shift of the corresponding spectrum. Field shift is caused by differences in the nuclear charge radius. Mass shift is generally proportional to the change of relative mass between isotopes, while field shift is mainly related to the differences in mean square nuclear charge distribution between isotopes.[25,26] Due to mass shift and field shift contributions, the IS for transition $i$ between isotopes $A$ and $A'$ can be written as

$$\begin{aligned}\delta\nu_{\mathrm{IS}}^{A,A'} &= \delta\nu_{\mathrm{MS}}^{A,A'} + \delta\nu_{\mathrm{FS}}^{A,A'} \\ &= M \cdot \frac{m_{A'} - m_A}{m_{A'} \cdot m_A} + F \cdot \delta\langle r^2\rangle^{A,A'}, \end{aligned} \tag{1}$$

where $M$ and $F$ are the mass and field shift constants, respectively, depending on the investigated transition; $\delta\langle r^2\rangle^{A,A'} = \langle r^2\rangle^{A} - \langle r^2\rangle^{A'}$ is the difference of the mean squared nuclear charge radii, which is identical in transitions but may contain quantities beyond the current nuclear theory of the SM. Thus, $\delta\langle r^2\rangle^{A,A'}$ can be eliminated by comparing two transitions $i$ and $j$.[7] Here, $\mu^{A,A'} = m_A^{-1} - m_{A'}^{-1}$ is the change in inverse nuclear mass,[15,16] a modified IS $\delta\nu_{\mathrm{IS}}^{A,A'}/\mu^{A,A'}$ can be written as

$$\frac{\delta\nu_i^{A,A'}}{\mu^{A,A'}} = \frac{F_i}{F_j} \cdot \frac{\delta\nu_j^{A,A'}}{\mu^{A,A'}} + \left(M_i - M_j \cdot \frac{F_i}{F_j}\right). \tag{2}$$

Therefore, King-plot analysis is taken, which represents the IS correlation analysis of two transitions.[1]

**Table 1.** The resonance frequency shift of isotope pairs in the $6s\,^2S_{1/2} \leftrightarrow 6p\,^2P_{1/2}$ and $5d\,^2D_{3/2} \leftrightarrow 6s\,^3[3/2]_{1/2}$ transitions of Yb$^+$.

| Isotopes $A$ | Resonance frequency $\nu_{369}$ (THz) | | | Resonance frequency $\nu_{935}$ (THz) | | |
|---|---|---|---|---|---|---|
| | This work | Hur *et al.*[16] | McLoughlin *et al.*[21] | This work | Hur *et al.*[16] | McLoughlin *et al.*[21] |
| 176 | 811.290297(12) | 811.290250(100) | 811.290310(126) | 320.574483(8) | 320.574515(50) | 320.574490(70) |
| 174 | 811.291518(12) | 811.291460(100) | 811.291540(126) | 320.571996(8) | 320.572010(50) | 320.572010(70) |
| 172 | 811.292790(12) | 811.292740(100) | 811.292840(126) | 320.569370(8) | 320.569390(50) | 320.569410(70) |
| 170 | 811.294410(12) | 811.294390(100) | 811.294400(126) | 320.565894(8) | 320.565910(50) | 320.565930(70) |
| 168 | 811.296154(12) | 811.296110(100) | | 320.562170(8) | 320.562190(50) | |
| | Isotope shift (MHz) | | | | | |
| | $\delta\nu_{369}^{A,176}$ | | | $\delta\nu_{935}^{A,176}$ | | |
| 174 | 1221(6) | | | −2487(6) | | |
| 172 | 2493(6) | | | −5113(6) | | |
| 170 | 4113(6) | | | −8589(6) | | |
| 168 | 5857(6) | | | −12313(6) | | |

It is known that the mass shift is generally proportional to the change of relative mass, and assuming that the field shift is proportional to the mean square nuclear charge distribution between isotopes, then the IS of the same isotope pairs on two transitions is linear to each other in the King-plot analysis, named as King's linearity.[1]

Through this experiment, we obtained the resonance frequency shift of isotope pairs (174–176, 172–174, 170–172, 168–170) on the $6s\,^2S_{1/2} \leftrightarrow 6p\,^2P_{1/2}$ and $5d\,^2D_{3/2} \leftrightarrow 6s\,^3[3/2]_{1/2}$ transitions, as listed in Table 1. From these results, we deduce an overall uncertainty including 2 MHz for the WS8-2, 6 MHz for measuring error. By changing locking points at a ULE cavity more slightly and monitoring the corresponding atomic fluorescence changing with 17% level we finally improved the resonant frequency uncertainty to ±6 MHz. Since 369 nm is generated by triple frequency laser and we lock 1108 nm on the WS8-2, the error for wavelength meter is 6 MHz on the $6s\,^2S_{1/2} \leftrightarrow 6p\,^2P_{1/2}$ transition.

With mass shift and field shift contributions and based on Eqs. (1) and (2), we performed a King-plot analysis of the isotope shift of $^{168,170,172,174,176}\mathrm{Yb}^+$ on two transitions. Two-dimensional King plot is shown in Fig. 4. The King plot is thus marginally linear within our measurement uncertainty, and we can obtain $\frac{F_{935}}{F_{369}} = -2.44(0.07)$, $M_{935} - M_{369} \cdot \frac{F_{935}}{F_{369}} = 7.24(1.46)$ THz·u.

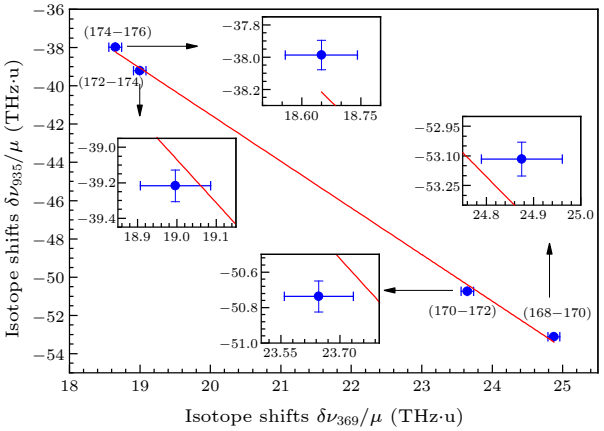


**Fig. 4.** Two-dimensional King plot of isotope $^{168,170,172,174,176}\mathrm{Yb}^+$. The horizontal coordinate shows the frequency shift of isotope pairs (174–176, 172–174, 170–172, 168–170) on the $6s\,^2S_{1/2} \leftrightarrow 6p\,^2P_{1/2}$ transition and the vertical coordinate shows the frequency shift of isotope pairs (174–176, 172–174, 170–172, 168–170) on the $5d\,^2D_{3/2} \leftrightarrow 6s\,^3[3/2]_{1/2}$ transition.

In summary, we have presented a feasible and precise method to measure isotope shifts of $^{168,170,172,174,176}\mathrm{Yb}^+$ on the $6s^2S_{1/2} \leftrightarrow 6p\,^2P_{1/2}$ and $5d\,^2D_{3/2} \leftrightarrow 6s\,^3[3/2]_{1/2}$ transitions. We successfully load five stable isotope single ytterbium ions using ablation technique and stably trapped them for a long time. The resonance frequency shift of the five stable isotopes ($A$ = 168, 170, 172, 174, 176) at 369 nm and 935 nm on the $6s\,^2S_{1/2} \leftrightarrow 6p\,^2P_{1/2}$ and $5d\,^2D_{3/2} \leftrightarrow 6s\,^3[3/2]_{1/2}$ transitions are obtained by recording frequencies from the wavelength meter within accuracy at megahertz. The interrogation lasers are locked on the wavemeter which is calibrated by a 729 nm clock laser of $^{40}\mathrm{Ca}^+$. The readout of the wavemeter is calibrated by comparing the fs-comb's readout frequency of the 1108 nm laser that was locked to a ULE cavity. The accuracy of the IS measurement on the $6s\,^2S_{1/2} \leftrightarrow 6p\,^2P_{1/2}$ and $5d\,^2D_{3/2} \leftrightarrow 6s\,^3[3/2]_{1/2}$ transitions has been improved by means of the ULE cavity and the fs-comb. Our method is simple, low-cost, and occupies a small space, which is easily applicable to other elements and other transitions. The resulting measurement provides a benchmark for tests of theoretical isotope shift calculations and also offers a step towards probing new physics via isotope shift spectroscopy. In future work, we plan to measure the absolute frequency on the accurate clock transition at ∼Hz level, then we can break the King's linearity and analyze the source of nonlinearity combined with theoretical calculations. Such searches are expected to set more stringent bounds between the SM and new physics and discover new physics beyond the SM, which can be used to detect dark matter and Bose force.

*Acknowledgments.* Supported by the National Natural Science Foundation of China (Grant Nos. 12204491 and 12121004), the National Basic Research Program of China (Grant No. 2021YFF0603801), Wuhan Young Talent Program (Grant No. R22H000106), the Natural Science Foundation of Hubei Province (Grant No. 2022CFA013), the CAS Youth Innovation Promotion Association (Grant Nos. Y201963 and 2018364), and CAS Project for Young Scientists in Basic Research (Grant No. YSBR-055).

# References

[1] King W H 1984 *Isotope Shifts in Atomic Spectra* (New York: Springer)
[2] Silverans R E, Lievens P, Vermeeren L, Arnold E, Neu W, Neugart R, Wendt K, Buchinger F, Ramsay E B, and Ulm G 1988 *Phys. Rev. Lett.* **60** 2607
[3] DeMille D, Doyle J M, and Sushkov A O 2017 *Science* **357** 990
[4] Knollmann F W, Patel A N, and Charles D S 2019 *Phys. Rev. A* **100** 022514
[5] Kalita M R, Behr J A, Gorelov A, Pearson M R, DeHart A C, Gwinner G, Kossin M J, Orozco L A, Aubin S, Gomez E, Safronova M S, Dzuba V A, and Flambaum V V 2018 *Phys. Rev. A* **97** 042507
[6] Safronova M S, Budker D, DeMille D, Jackson K D F, Derevianko A, and Clark C W 2018 *Rev. Mod. Phys.* **90** 025008
[7] Gorges C, Blaum K, Frömmgen N, Ch G, Hammen M, Kaufmann S, Krämer J, Krieger A, Neugart R, Sánchez R, and Nörtershäuser W 2015 *J. Phys. B* **48** 245008
[8] Gebert F, Wan Y, Wolf F, Angstmann C N, Berengut J C, and Schmidt P O 2015 *Phys. Rev. Lett.* **115** 053003
[9] Müller P, König K, Imgram P, Jörg K, and Nörtershäuser W 2020 *Phys. Rev. Res.* **2** 043351
[10] Solaro C, Meyer S, Fisher K, Berengut J C, Fuchs E, and Drewsen M 2020 *Phys. Rev. Lett.* **125** 123003
[11] Zhao X, Yu N, Dehmelt H, and Nagourney W 1995 *Phys. Rev. A* **51** 4483
[12] Imgram P, König K, Jörg K, Ratajczyk T, Müller R A, Surzhykov A, and Nörtershäuser W 2019 *Phys. Rev. A* **99** 012511

[13] Lybarger J W E, Berengut J C, and Chiaverini J 2011 *Phys. Rev. A* **83** 052509
[14] Manovitz T, Shaniv R, Shapira Y, Ozeri R, and Akerman N 2019 *Phys. Rev. Lett.* **123** 203001
[15] Counts I, Hur J, Aude C D P L, Jeon H, Leung C, Berengut J C, Geddes A, Kawasaki A, Jhe W, and Vuletić V 2020 *Phys. Rev. Lett.* **125** 123002
[16] Hur J, Aude C D P L, Counts I, Knyazev E, Caldwell L, Leung C, Pandey S, Berengut J C, Geddes A, Nazarewicz W, Reinhard P G, Kawasaki A, Jeon H, Jhe W, and Vuletić V 2022 *Phys. Rev. Lett.* **128** 163201
[17] Figueroa N L, Berengut J C, Dzuba V A *et al.* 2022 *Phys. Rev. Lett.* **128** 073001
[18] Allehabi S O, Dzuba V A, Flambaum V V, and Afanasjev A V 2021 *Phys. Rev. A* **103** L030801
[19] Flambaum V V, Geddes A J, and Viatkina A V 2018 *Phys. Rev. A* **97** 032510
[20] https://material-properties.org/
[21] McLoughlin J J, Nizamani A H, Siverns J D, Sterling R C, Hughes M D, Lekitsch B, Stein B, Weidt S, and Hensinger W K 2011 *Phys. Rev. A* **83** 013406
[22] Brewer S M, Chen J S, Hankin A M, Clements E R, Chou C W, Wineland D J, Hume D B, and Leibrandt D R 2019 *Phys. Rev. Lett.* **123** 033201
[23] Shao H, Wang M, Zeng M, Guan H, and Gao K 2018 *J. Phys. Commun.* **2** 095019
[24] Bian W, Huang Y, Guan H, Liu P, Ma L, and Gao K 2016 *Rev. Sci. Instrum.* **87** 063121
[25] Johnson W R 2007 *Atomic Structure Theory* (Berlin: Springer-Verlag)
[26] Heilig K and Steudel A 1974 *At. Data Nucl. Data Tables* **14** 613